Discovering the Radiation Biomarkers in the Plasma of Total-Body Irradiated Leukemia Patients

Authors: Gabriela, Rydlova, Vera, Vozandychova, Pavel, Rehulka, Helena, Rehulkova, Igor, Sirak, et al.

Source: Radiation Research, 201(5) : 418-428

Published By: Radiation Research Society

URL: https://doi.org/10.1667/RADE-23-00137.1

RADIATION RESEARCH **201**, 418–428 (2024)
0033-7587/24 $15.00

DOI: 10.1667/RADE-23-00137.1

Discovering the Radiation Biomarkers in the Plasma of Total-Body Irradiated Leukemia Patients

Rydlova Gabriela,[a,d] Vozandychova Vera,[b] Rehulka Pavel,[b] Rehulkova Helena,[c] Sirak Igor,[e] Davidkova Marie,[f] Markova Marketa,[g] Myslivcova-Fucikova Alena,[d] Tichy Ales[a,1]

[a] Department of Radiobiology, [b] Department of Molecular Biology and Pathology, and [c] Department of Toxicology, Faculty of Military Health Sciences, University of Defence, Hradec Králové, Czech Republic; [d] Department of Biology, Faculty of Natural Sciences, University of Hradec Králové, Czech Republic, Hradec Králové, Czech Republic; [e] Department of Oncology and Radiotherapy and 4th Department of Internal Medicine - Haematology, University Hospital, Hradec Kralove, Czech Republic; [f] Department of Radiation Dosimetry, Nuclear Physics Institute of the Czech Academy of Sciences, Prague, Czech Republic; [g] Department of Haematology and Blood Transfusion, University Hospital Na Bulovce, Prague, Czech Republic

Rydlova G, Vozandychova V, Rehulka P, Rehulkova H, Sirak I, Davidkova M, Stastna Markova M, Myslivcova-Fucikova A, Tichy A. Discovering the Radiation Biomarkers in the Plasma of Total-Body Irradiated Leukemia Patients. Radiat Res. 201, 418–428 (2024).

The increased risk of acute large-scale radiological exposure for the world's population underlines the need for optimal radiation biomarkers. Ionizing radiation triggers a complex response by the genome, proteome, and metabolome, all of which have been reported as suitable indicators of radiation-induced damage in vivo. This study analyzed peripheral blood samples from total-body irradiation (TBI) leukemia patients through mass spectrometry (MS) to identify and quantify differentially regulated proteins in plasma before and after irradiation. In brief, samples were taken from 16 leukemic patients prior to and 24 h after TBI (2 × 2.0 Gy), processed with Tandem Mass Tag isobaric labelling kit (TMTpro-16-plex), and analyzed by MS. In parallel, label-free relative quantification was performed with a RP-nanoLC-ESI-MS/MS system in a Q-Exactive mass spectrometer. Protein identification was done in Proteome Discoverer v.2.2 platform (Thermo). Data is available via ProteomeXchange with identifier PXD043516. Using two different methods, we acquired two datasets of up-regulated (ratio ≥ 1.2) or down-regulated (ratio ≤ 0.83) plasmatic proteins 24 h after irradiation, identifying 356 and 346 proteins in the TMT-16plex and 285 and 308 label-free analyses, respectively (P ≤ 0.05). Combining the two datasets yielded 15 candidates with significant relation to gamma-radiation exposure. The majority of these proteins were associated with the inflammatory response and lipid metabolism. Subsequently, from these, five proteins showed the strongest potential as radiation biomarkers in humans (C-reactive protein, Alpha amylase 1A, Mannose-binding protein C, Phospholipid transfer protein, and Complement C5). These candidate biomarkers might have implications for practical biological dosimetry.

[1] Corresponding author: Assoc. Prof. Ales Tichy, PharmD., PhD., Department of Radiobiology, Faculty of Military Faculty of Medicine, University of Defence, Trebesska 1575, 500 01 Hradec Králové, Czech Republic; email: ales.tichy@unob.cz.

INTRODUCTION

The threat of radiological incidents has been increasing throughout the past years; therefore, it is to be expected that a large section of the world's population will be exposed to ionizing radiation at one point or another (*1*). In such circumstances, it becomes necessary to rapidly classify and separate the exposed and non-exposed individuals, and to estimate the absorbed radiation dose (*2*). The biological effects of radiation exposure depend on the dose rate, the physiological state of the cells, and exposure level (*3*). It must be highlighted that both low and high doses cause health issues after said exposure (*4*). In these type of accidents, biological dosimetry is crucial for an effective triage (*5*) and treatment classification (*6*) of the victims.

In this regard, biological dosimetry exploits radiation biomarkers present in blood, urine, hair, sputum, nails, etc. (*7*). Therefore, these biomarkers then become necessary for the prediction of deterministic and stochastic effects (e.g. cancer, genetic alterations, etc.) (*3*) and should be indicative of unique changes in the organism due to exposure to radiation and the following response which, regardless of either the physiological or medical condition of the afflicted, should be the same (*6*).

Several studies have been made in animals such as mice (*8*), rats, minipigs (*9*), and non-human primates (*10*), as exposing healthy human volunteers to radiation is unethical and dangerous (*11*). Therefore, research studies can only be performed on individuals accidently exposed to ionizing radiation or on patients undergoing radiotherapy, with appropriate human use approvals (*12*, *13*).

The gold standard for biological dosimetry diagnosis is based on the dicentric chromosome assay (DCA) (*14*), which can be used for retrospective dose assessment (*15*). This method is highly specific because dicentric chromosomes are primarily induced by radiation (*16*). However, it is also time consuming, labor intensive (*17*). genomics (*18*) and metabolomics (*13*) biomarkers can provide valuable insight concerning radiation exposure, and the proteomics

field has proven its important role in biodosimetry too (*19*). Hence, novel "-omics" based platforms have become appealing complementary approaches to the golden standard.

In this paper, we describe a unique proteomics study performed on a cohort of 16 leukemia patients undergoing total-body irradiation (TBI), applying a mass-spectrometry (MS) approach to analyze radiation-induced changes in the plasma proteome and identifying potential biomarkers of total-body gamma-irradiation.

MATERIALS AND METHODS

Sample Collection and Preparation

A total of 16 leukemia patients undergoing TBI were included in this study after providing their informed consent. The study meets the approval requisites of the ethics committee of the University Hospital Bulovka, Prague. In the period of 2015–2019, blood samples were collected from twelve males and four females (Table 1) aged 19 to 58 years (median 38.0) received TBI (two doses of 2.0 Gy). Patients were irradiated by standard C-arm linear accelerator Versa HD (Elekta Solutions AB, Stockholm, Sweden) using homogenous 6MV X-ray beams with a dose rate of 3 Gy/min. The doses to the patients were delivered using sweeping beam technique. In this method, the patient lies on a special couch situated on the floor perpendicular to the target-gun axis at a source-skin distance of 200 cm and the linear accelerator gantry is sweeping over the patient with jaws wide open. To reach the TBI dosimetric recommendations regarding dose homogeneity, patients were irradiated by two arcs— the first arc in a supine and the second arc in a prone position. Moreover, to keep the constant source-to-patient distance we used the U-like curved couch. Delivered doses were verified using in vivo measurements at several points on the skin in both positions – prone and supine.

As a comparative control, 15 samples were collected from healthy donors, i.e., six females and nine males aged 25 to 46 years (median 36.0). All the samples were collected at two different intervals: prior to and 24 h after irradiation. The samples from the control group were taken in a similar interval. The samples were collected into vacuum tubes (BD P100, Becton Dickinson, Franklin Lakes, NJ) during the early morning and processed within 1 h after collection. The plasma was separated by centrifugation (2,500 × *g* for 20 min at 22°C), from which ~3.5 ml was aliquoted and stored at –80°C.

A relative proteomic quantitation of the samples was done using two label free quantitation and TMTpro16 isobaric labelling. In both cases, the samples were digested and directly analyzed through LC-MS (label-free experiment). In contrast, the peptides had to be labelled with a stable isotope in the TMTpro16 analysis, chromatographically fractionated, and analyzed through LC-MS. The obtained data was pooled and relative protein abundance was determined through bioinformatics analyses. The patients were split equally in two groups, i.e., LFQ1 or TMT1 and LFQ2 or TMT2, each including two sample sets (0 h and 24 h postirradiation). A direct comparison was made between the obtained data sets.

Prior to proteomic analysis, the samples were centrifuged in 0.22 μm spin filter tubes Ultrafree-MC (Amicon, Millipore Corporation, Bedford, MA) at 10,000 × *g* for 5 min at 4°C. Thereafter, High Select™ Top14 Abundant Protein Depletion Mini Spin Columns (Thermo Fisher Scientific, Waltham, MA) were used to remove the most abundant proteins in human plasma (i.e., albumin, IgG, antitrypsin, IgA, transferrin, haptoglobin, fibrinogen, alpha-2-macroglobulin, alpha-1-acid glycoprotein, IgM, apolipoprotein A1, apolipoprotein A2, complement C3 and transthyretin).

Protein concentration was determined using the BCA and tryptophan fluorescence-based protein quantification methods (*20*), making a comparison between them for greater accuracy. An SDS-PAGE was performed to assess the efficiency and quality of the depletion step. Afterwards, 50 μg protein were used in the quantitative proteomic analyses.

TABLE 1
Overview of 16 Leukemia Patients

Patient code	Sex	Age	Diagnosis	Total dose (Gy)
TBI 2 B	M	28	ALL	3.72
TBI 6 B	M	56	ALL	4.49
TBI 7 B	F	39	ALL	4.18
TBI 8 B	M	46	ALL	4.38
TBI 9 B	M	31	ALL	4.65
TBI 10 B	M	56	ALL	4.46
TBI 11 B	M	53	ALL	4.41
TBI 13 B	F	54	ALL	4.42
TBI 18 B	M	19	ALL	4.12
TBI 19 B	M	54	ALL	4.28
TBI 21 B	M	46	ALL	3.84
TBI 23 B	M	53	ALL	4.19
TBI 24 B	F	58	ALL	4.33
TBI 25 B	F	46	ALL	3.94
TBI 27 B	M	58	ALL	4.89
TBI 29 B	M	30	ALL	3.87

Notes. Samples from total-body irradiation leukemia patient. The overview shows 16 leukemia patients code, sex, age, diagnosis and the total dose of ionizing radiation received. Abbreviations: TBI, total-body irradiation; M, male; F, female; ALL, acute lymphoblastic leukemia

Elaborating further, the plasma aliquots were diluted up to 250 μl with 10 mM phosphate buffer (Sigma-Aldrich, St. Louis, MO) and 30 μl 10% SDS (Sigma-Aldrich, St. Louis, MO) were added. The proteins were denatured at 95°C for 3 minutes. After addition of 30 μl 1M triethylammonium bicarbonate (Sigma-Aldrich, St. Louis, MO) and 15 μl 200 mM tris(2-carboxyethyl)phosphine hydrochloride (Sigma-Aldrich, St. Louis, MO) the proteins were reduced for 60 min at 60°C. The mixture was alkylated with 15 μl 375 mM iodoacetamide (Sigma-Aldrich, St. Louis, MO) for 30 min at room temperature. The proteins were precipitated with the addition of 6 volumes acetone and incubated at –20°C overnight. The precipitated proteins were centrifuged (8,000 × *g*) for 10 min at 4°C, the supernatant was removed and the protein pellet dried for 2 min in vacuum centrifuge.

The protein pellet was redissolved in 70 μl water, 10 μl 10% sodium deoxycholate (Sigma-Aldrich, St. Louis, MO) and 10 μl 1M triethylammonium bicarbonate (Sigma-Aldrich, St. Louis, MO) in a sonicator. The proteins were digested by adding 10 μl of trypsin (Promega, Madison, WI) (1:30 w/w) and incubating at 37°C overnight. The samples were acidified with the addition of 20 μl 10% trifluoroacetic acid (TFA) (Sigma-Aldrich, St. Louis, MO), centrifuged (4,000 × *g*) for 10 min and the supernatant was transferred to a clean 1.5 ml tube. The pellet was washed with 100 μl 1% TFA and centrifuged (4,000 × *g*, 2 min). The wash solution was pooled with the sample's supernatant. Later, 750 μl ethyl acetate (Sigma-Aldrich, St. Louis, MO) were added to this solution, vortexed for 30 s and centrifuged (10,000 × *g*, 1 min). The upper organic layer was removed. This step was repeated 4 times. The remaining aqueous layer containing the digested peptides was dried in a vacuum centrifuge. The samples were redissolved in 400 μl 2% acetonitrile (Sigma-Aldrich, St. Louis, MO)/0.1% TFA (v/v) and purified using C18 solid-phase extraction cartridges (3M™ Empore™, St. Paul, MN) according to manufacturer instructions and using double elution with 150 μl 50% acetonitrile/0.1% TFA (v/v). From this, 5 μg peptides were taken, dried in a vacuum centrifuge and redissolved in 20 μl 2% acetonitrile/0.1% TFA (v/v) for the label-free LC-MS quantitation analysis. The remaining eluent was dried in vacuum centrifuge, redissolved in water, and 25 μg of each sample were taken for the TMTpro16 labelling analysis, where 10 μl 1 M triethylammonium bicarbonate were added to each sample, and water was added to a final volume of

100 µl. These samples were dissolved in 40 µl anhydrous acetonitrile (5 min with occasional vortexing), and 20 µl of the labelling solution added and briefly vortexed. The samples were incubated 60 min at 25°C. The reaction was quenched with the addition 5 µL of 5% hydroxylamine and incubation for 15 min. The TMTpro16 labelled sample were split into 28 fractions, vacuum dried and analyzed through LC-MS.

LC-MS Analysis

The samples were dissolved in 20 µl 2% acetonitrile/0.1% TFA (v/v) and 1 µl of the sample was analyzed using a gradient nanoLC system with UV detection (UltiMate 3000 HPLC system (Dionex) as previously described (*21*). The optimized samples were then used for LC-MS analysis in an UltiMate 3000 RSLC-nano HPLC (Dionex) coupled with QExactive (Thermo Fisher Scientific) (*21*). Data acquisition was done with the Xcalibur (v4.2.47) and Tune control (v2.11.0.3006) software. The label-free quantitation settings were as follows: full MS scan (350–1650 m/z) at 70,000 FWHM with maximum filling time 100 ms and AGC target 1E6; top 12 precursors in MS/MS at 17,500 FWHM with isolation window 1.6 m/z, fixed first mass at 140 m/z, maximum filling time 100 ms and AGC target 1E5. The instrument settings for TMT quantitation analysis were adjusted as follows: full MS scan (400–1650 m/z) at 70,000 FWHM with maximum filling time 100 ms and AGC target 3E6; top 10 precursors in MS/MS at 35,000 FWHM with isolation window 1.2 m/z, fixed first mass at 110 m/z, maximum filling time 250 ms and AGC target 2E5.

Bioinformatics

The spectra files were processed in the Proteome Discoverer software (Thermo Fisher Scientific, v2.4.1.15), through which the proteins present in the samples could be identified and quantified (i.e., relative protein abundance). The data processing workflow contained a spectrum selector, non-fragment filter, top N peaks filter, precursor detector, SequestHT search engine, Percolator validator, Spectrum Confidence Filter, SequestHT search engine and Percolator validator (second round search) nodes. The parameters for the first SequestHT database search were: protein database - UniProt human reference proteome UP000005640 (May 1, 2023); enzyme - trypsin; maximum missed cleavage sites - 1; min. peptide length - 7; precursor mass tolerance - 10 ppm; fragment mass tolerance - 0.02 Da; weight of b- and y-ions - 1; static modifications - Carbamidomethyl/+57.021 (C); dynamic modifications - Oxidation/+15.995 Da (M); dynamic modifications (protein terminus) - Acetyl/+42.011 Da (N-terminus), Met-loss/–131.040 Da (M), Met-loss+Acetyl/–89.030 Da (M). The obtained data was then processed in the consensus workflow: PSM Grouper, Peptide Validator, Protein and Peptide Filter (two peptides with strict target FDR 0.01), Protein Scorer, Protein FDR Validator, Protein Grouping, Protein in Peptide Annotation, Modification Sites, Protein Annotation and Protein Marker nodes. Regarding the label-free quantitation analysis, a Minora Feature Detector node was used in the processing workflow and Feature Mapper and Precursor Ions Quantifier (with pairwise computed protein ratio and background-based t-testing) nodes were applied in the consensus workflow. On the other hand, the TMTpro16 labelling experiment used a Reporter Ions Quantifier node in the processing workflow and Reporter Ions Quantifier node in the consensus workflow (with pairwise computed protein ratio and background-based t-testing). A nested experiment design was applied in this study because the samples were collected twice from identical patients at two different time points (0 h and 24 h). Gene ontology analysis was performed with the Metascape program.

The raw MS data, as well as the processed identification results, have been deposited in the ProteomeXchange Consortium via the PRIDE partner repository with the dataset identifier PXD043516 (DOI: 10.6019/PXD043516) (*22*).

RESULTS

According to the capacity of the isobaric TMT labels, 16 plex was used in our study, where each of the 8 samples were divided into two halves (0 G and 24 h). The radiation dose was identical for all patients (2×2 Gy). The samples were grouped according to sex and randomized. The first group (TMT1) contained only male donors whereas that the second group (TMT2) had patients of both sexes. The groups with equal sample distribution were retained when implementing the LFQ method (LFQ1 and LFQ2) and, based on the results from the Proteome Discoverer analytical program, the individual data from LFQ and isobaric TMT labelling were compared with each other.

This approach allowed the identification of a large number of proteins, from which suitable candidates were selected based on a set of specific criteria. These were maintained for both groups and the LFQ and TMT methods. First, we compared the abundance ratio with the corresponding P value. In the control group, the difference for individual proteins determined at time 0 and 24 h ranged from 1.21 to 0.89, thus establishing this range as a threshold. In the TBI patients, any observed change would only be considered as significant if their value was over 1.21 or less than 0.89-fold ($P \leq 0.05$). A comparison between leukemia and control samples was made at 0 h to remove those proteins directly associated with the disease from further analysis. Contaminants, such as keratin, and several depleted abundant proteins were discarded.

The analysis of the TMT1 data resulted in the identification of 356 proteins, 78 of which had an expression fold-change after irradiation; of these, only 19 proteins displayed statistical significance ($P \leq 0.05$) (Table 2). The TMT2 dataset identified 346 proteins, of which 91 showed an expression fold-change after irradiation; of these, 29 possessed statistical significance (Table 3).

Based on the LFQ1 experiment we identified 285 proteins, of which 65 showed an expression fold-change after irradiation and out of which 23 were statistically significant (Table 4). Finally, the LFQ2 experiment identified 308 proteins, 85 of which showed an expression fold-change after irradiation and out of which 45 were statistically significant (Table 5).

The candidates that met the specified criteria were selected from both TMT and LFQ data sets, totaling 15 candidates in the first screening stage, being later reduced to only five. Importantly, the selected candidates were included previously reported radiation-responsive proteins and others involved in the immune response, including C-reactive protein (CRP), Alpha amylase 1A (AMY1A), Phospholipid transfer protein (PLPT), Complement C5 (C5), and Mannose-binding protein C (MBL; Tables 6a and 6b). The abundance ratio and P value showed a greater significance in the second group of patients. However, the difference between irradiated and non-irradiated samples was significant in all 16 samples. When comparing the

TABLE 2
Potential Candidates from TMT1 Dataset

Description	Abundance ratio: (24 h)/(0 h)	Abundance ratio P value: (24 h)/(0 h)
Platelet-activating factor acetylhydrolase	2.022	9,03E-05
Carbonic anhydrase 2	1.917	3,27E-04
Tsukushi	1.911	3,49E-04
Protein S100-A6	1.883	4,89E-04
Peroxiredoxin-2	1.849	7,38E-04
Lymphatic vessel endothelial hyaluronic acid receptor 1	1.848	7,41E-04
Ficolin-2	1.795	1,39E-03
Carbonic anhydrase 1	1.762	2,03E-03
Mannose-binding protein C	1.651	7,15E-03
Alpha-amylase 1A	1.618	1,01E-02
Prenylcysteine oxidase 1	1.602	1,21E-02
Protein S100-A9	1.549	2,12E-02
Putative annexin A2-like protein	1.475	4,45E-02
Glyceraldehyde-3-phosphate dehydrogenase	1.468	4,75E-02
Catalase	1.463	4,97E-02
Multiple inositol polyphosphate phosphatase 1	0.749	3,71E-02
Chromogranin	0.693	1,08E-02
Protein disulfide-isomerase A3	0.586	3,69E-04
Insulin-like growth factor lI	0.418	2,01E-08

Notes. The 19 candidates were selected based on the criteria from TMT1 dataset. Data show the best protein candidates with the most significant change levels after irradiation in plasma ($P < 0.05$).

TABLE 3
Potential Candidates from TMT2 dataset

Description	Abundance ratio: (24 h)/(0 h)	Abundance ratio P-Value: (24 h)/(0 h)
Alpha-amylase 1A	3.328	1,80E-13
C-reactive protein	2.100	1,05E-05
Trypsin-1	1.894	1,81E-04
Lysosome-associated membrane glycoprotein 1	1.880	2,20E-04
Calmodulin-like protein 5	1.815	5,24E-04
Prenylcysteine oxidase 1	1.679	3,02E-03
Retinoic acid receptor responder protein 2	1.594	8,49E-03
Complement C5	1.586	9,27E-03
Oncostatin-M-specific receptor subunit beta	1.581	9,83E-03
Adenosine deaminase 2	1.549	1,43E-02
Serum amyloid P-component	1.545	1,49E-02
Phospholipid transfer protein	1.494	2,65E-02
Ecto-ADP-ribosyltransferase 3	1.490	2,78E-02
Coagulation factor IX	1.475	3,30E-02
Phosphatidylethanolamine-binding protein 4	1.472	3,40E-02
Dermcidin	1.469	3,49E-02
Ankyrin-1	0.775	4,55E-02
Lysozyme C	0.770	4,11E-02
Carbonic anhydrase 2	0.751	2,74E-02
CD166 antigen	0.735	1,89E-02
Protein S100-A9	0.732	1,766-02
Protein S100-A8	0.722	1,38E-02
Platelet factor 4 variant	0.721	1,35E-02
Hemoglobin subunit gamma-1	0.718	1,26E-02
Carbonic anhydrase 1	0.688	5,54E-03
Tubulin beta-6 chain	0.687	5,42E-03
Thrombospondin-1	0.630	8,37E-04
Protein S100-A6	0.566	5,59E-05
Platelet basic protein	0.562	4,68E-05

Notes. The 29 candidates were selected based on the criteria from TMT2 dataset. Data show the best protein candidates with the most significant change levels after irradiation in plasma ($P < 0.05$).

results from both methods, we concluded that the resulting abundance ratio values were, with a few exceptions, very similar.

Protein-Protein Interaction

The candidate proteins were evaluated concerning their biological function. In this manner, several radiation-induced signaling pathways were identified (Fig. 1). These pathways could be associated with opsonization, the complement system, and insulin-like growth factor (IGF) regulation. In addition, carbohydrate metabolism and cell proliferation were also dysregulated.

DISCUSSION

The current biological dosimetry techniques are still reliant on the gold-standard, i.e., the analysis of dicentric chromosomes (DCA), which is used to determine radiation dose. Although the DCA is reliable and reproducible, it is also time-consuming and very laborious and therefore not fully satisfactory for incidents involving mass casualty. In these scenarios, rapid assays are needed (*23*). Therefore, the present study sought to identify radiation exposure biomarkers that might complement already established biodosimetric methods (*24*, *25*).

The data analysis identified five protein candidates with highly significant expression change after irradiation, i.e., CRP, AMY1A, PLPT, C5 and MBL. These proteins participate in metabolic pathways known to be altered through radiation exposure (*26*, *27*).

CRP, along with pro-inflammatory cytokines, plays an important role in innate immunity, immunoglobulin receptor binding, opsonization, complement activation, and inflammation (*28*). The latter has an essential function in several pathogenic processes, such as atherosclerosis, which is caused by radiation (*29*). Further, CRP has been classified as a risk factor in cardiovascular disease (CVD),

TABLE 4
The Potential Candidates from LFQ1 Dataset

Description	Abundance Ratio: (24 h)/(0 h)	Abundance ratio P value: (24 h)/(0 h)
Cofilin-1	100.00	1,00-17
Neutrophil defensin 1	100.00	1,00E-17
Talin-1	100.00	1,00E-17
Peptidyl-prolyl cis-trans isomerase A	9.280	1,00E-17
14-3-3 protein zeta/delta	2.958	2,97E-07
Flavin reductase (NADPH)	2.587	6,94€E-06
Filamin-A	2.223	1,57E-04
Hemoglobin subunit delta	1.974	1,28E-03
Serglycin	1.964	1,39E-03
Platelet factor 4	1.889	2,58E-03
Tropomyosin alpha-4 chain	1.857	3,37E-03
Adenosine deaminase 2	1.788	5,88E-03
Lactotransferrin	1.755	7,69E-03
Peroxiredoxin-2	1.676	1,43E-02
Catalase	1.662	1,600E-02
Carbonic anhydrase 1	1.556	3,57E-02
Ficolin-2	1.512	4,94E-02
Pyruvate kinase PKM	0.604	1,85E-02
Immunoglobulin heavy constant alpha 2	0.587	1,28E-02
Tyrosine-protein kinase ITK/TSK	0.349	7,58E-07
A disintegrin and metalloproteinase with thrombospondin motifs 13	0.244	3,20E-11
Serpin B3	0.01	1,00E-17
Tubulin alpha-1A chain	0.01	1,00E-17

Notes. The 23 candidates were selected on the basis of the criteria from LFQ1 dataset. Data show the best protein candidates with the most significant change levels after irradiation in plasma ($P < 0.05$).

playing a direct role in their development (*30*). In this regard, previous epidemiological studies suggest that the exposure to low and medium doses of radiation could increase the risk of CVD, whereas that high doses accelerate the development of atherosclerosis.

The increase in CRP levels after irradiation was confirmed in a study by Cenigz et al., where 51 patients diagnosed with endometrial cancer were irradiated with a dose of 50.4 Gy. The post-irradiation values increased up to two-fold when compared to pre-radiotherapy (*26*). Similar results were observed by Ki et al. and Ossectrova et al., thus supporting the results hereby observed (*31*, *32*).

AMY1A is another of the top candidates found in this study. This protein, amyolytic enzyme catalyzing alpha-1,4-glycosidic, binds to starch and other related alfa glucans (*33*). It is systemically expressed, including the salivary glands, which are affected by TBI, inducing the increased concentration of amylase in serum. Therefore, a correlation between serum amylase and the radiation dose received was proposed and an early biomarker of salivary gland

TABLE 5
The Potential Candidates from LFQ2 Dataset

Description	Abundance Ratio: (24 h)/(0 h)	Abundance ratio P value: (24 h)/(0 h)
Alpha-amylase 1A	100.00	1,00E-17
Serpin B3	100.00	1,00E-17
Putative annexin A2-like protein	24.726	1,00E-17
Desmoglein-2	14.251	1,00E-17
Roundabout homolog 4	13.886	1,00E-17
Protein S100-A12	11.557	1,98E-02
Serpin B12	10.132	1,00E-17
Desmocollin-1	7.586	8,35E-13
Nesprin-1	2.590	7,47E-05
Peroxiredoxin-1	2.589	7,47E-05
C-reactive protein	2.049	1,16E-04
Dermcidin	1.910	5,06E-04
Cystatin-A	1.812	2,96E-02
Calmodulin-like protein 5	1.751	2,60E-03
Lipopolysaccharide-binding protein	1.585	1,33E-02
Apolipoprotein F	1.543	1,97E-02
Phospholipid transfer protein	1.543	2,19E-05
Thyroxine-binding globulin	1.527	2,29E-02
Complement C5	1.494	3,11E-02
Corticosteroid-binding globulin	1.461	4,16E-02
Protein S100-A8	0.689	4,54E-02
Spectrin beta chain, erythrocytic	0.684	4,14E-02
Immunoglobulin heavy constant gamma 1	0.67	3,14E-02
Desmoglein-1	0.668	2,99E-02
Lysozyme C	0.654	2,22E-02
Fumarylacetoacetase	0.636	1,48E-02
Glyceraldehyde-3-phosphate dehydrogenase	0.623	1,08E-02
Multivesicular body subunit 12B	0.622	1,07E-02
Hemoglobin subunit beta	0.621	1,03E-02
Serpin A11	0.57	9,09E-03
Hemoglobin subunit alpha	0.558	1,73E-03
Serum amyloid A-2 protein	0.501	2,04E-04
Band 3 anion transport protein	0.472	5,49E-05
Platelet basic protein	0.456	2,43E-05
Carbonic anhydrase 2	0.438	8,91E-06
Platelet factor 4	0.424	3,92E-06
Serum amyloid A-1 protein	0.424	3,94E-06
Hemoglobin subunit delta	0.398	7,29E-07
Thrombospondin-1	0.392	4,66E-07
Flavin reductase (NADPH)	0.181	2,85E-11
Collagen alpha-1I) chain	0.103	1,00E-17
Phosphoglycerate kinase 1	0.102	1,00E-17
Vinculin	0.073	1,00E-17
Nucleoside diphosphate kinase A	0.01	1,00B-17
Transketolase	0.01	1,00e-17

Notes. The 45 candidates were selected on the basis of the criteria from LFQ2 dataset. Data show the best protein candidates with the most significant change levels after irradiation in plasma ($P < 0.05$).

TABLE 6A
Candidates Selected from TMT1 and LFQ1 Datasets

		TMT1		LFQ1	
Accession	Description	Abundance ratio: (24 h)/(0 h)	Abundance ratio P value: (24 h)/(0 h)	Abundance ratio: (24 h)/(0 h)	Abundance ratio P value: (24 h)/(0 h)
P02741	C-reactive protein	1.351	1,39E-01	1.455	7,47E-02
PODUB6	Alpha-amylase 1A	1.618	1,01E-02	1.023	9,01E-01
P11226	Mannose-binding protein C	1.651	7,15E-03	1.274	2,46E-01
P55058	Phospholipid transfer protein	1.453	5,47E-02	1.113	6,03E-01
P01031	Complement CS	1.337	1,56E-01	1.206	3,69E-01
P24592	Insulin-like growth factor-binding protein 6	1.287	2,34E-01	1.438	8,37E-02
P04114	Apolipoprotein B-100	1.316	1,866-01	1.246	2,93B-01
Q13790	Apolipoprotein F	1.015	8,06E-01	1.402	1,08E-01
P61626	Lysozyme C	0.955	5,40E-01	0.744	1,68E-01
P18428	Lipopolysaccharide-binding protein	0.963	5,72E-01	1.219	3,43E-01
Q01459	Di-N-acetylchitobiase	1.133l	6,77E-01	1.25	2,85E-01
O75636	Ficolin-3	1.278	2,52E-01	1.096	6,53E-01
P29622	Kallistatin	1.208	4,22E-01	1.131	5,50E-01
P04070	Vitamin K-dependent protein C	1.404	8,66E-02	1.177	4,33E-01
Q15848	Adipoctin	1.233	3,54E-01	1.201	3.80E-01

Notes. Overview of 15 candidates selected from TMT1 and LFQ1 datasets based on ratio of the values at 0 h and 24 h postirradiation. The threshold value of abundance ratio was set as higher than 1.21 or lower than 0.89-fold ($P \leq 0.05$).

damage was established (*34*). Previous studies showed that amylase production increased under the local irradiation of the salivary glands, being as high as 80-fold. However, TBI caused little to no change in amylase production (*35*). On the other hand, another study conducted on rhesus macaques revealed a consistent increment of AMY1A in plasma 1 day after TBI (*36*), which is consistent with our observations.

Another candidate, PLPT, is a major component of the cell membrane, having important biological functions such as phospholipid transport (*37*). Membrane lipids (and especially phospholipids containing polyunsaturated fatty acids) are very susceptible to the presence of reactive oxygen species (ROS), as it can disrupt the membrane and induce changes in fluidity and permeability, ion transport alterations, and inhibit cell metabolism (*27*). Radiation exposure leads to the oxidative damage of phospholipids caused by free oxygen radicals (*38*). The alternation in membrane function and phospholipid metabolism was suggested as a potential marker of radiation exposure in a previous report (*39*), which is supported by the findings revealed in this study, where a >1.5-fold increase in plasma PLPT levels was observed.

The fourth candidate, C5, is part of the complement system, participating in inflammatory processes along with CR1 and CR3 and functioning as an enzymatic mediator. Complement system proteins are normally inactive until sequentially activated by a series of chain reactions (*40*). The IL-6 cytokine activates C5, which produces a potent anaphylatoxin via receptor C5aR. This leads to pathogen lysis, inflammation, and cell damage (*41*). The association between the increased C5aR levels in response to IL-6 has been demonstrated during toxic liver injury (*42*). Promoting hepatocyte regeneration is desirable, as radiation exposure can cause serious damage to liver tissue (*43*), whose significant recovery through C5a has been previously reported in mice (*44*). On the other hand, tumor-associated dendritic cells also exhibit increased C3a and C5aR1 expression after radiotherapy (*45*). Further, a clear relation between irradiation and the complement system was described Surace et al. (*46*). Radiation exposure results in the production of anaphylatoxins (C3a and C5a), which then stimulate the adaptive immunity and contribute to the elimination of cancer cells (*46*). Radiotherapy of mouse lung carcinoma upregulated C5aR1 expression in $CD8^+$ T cells (*47*), which supports our findings.

Our results also demonstrated an increment in C5 expression up to 1.5-fold when compared to control samples, underlying its importance in the response to TBI.

The last one is MBL, whose level can be increased due to radiation exposure, thus activating the complement lectin pathway (*47*). Since the complement system is initiated by MBL, its relevance to radiation-induced response is obvious.

The level of MBL in serum after the total-body irradiation of mice (11 Gy) was significantly higher than before irradiation (*48*), again, confirming the results of our study. Similar increase was found in another work, where the mice were irradiated with a dose of 3 Gy (*49*).

During this research, other radiation-biomarker candidates were identified. Unfortunately, the obtained P value lacked any statistical significance. Among these, we identified proteins such as insulin-like growth factor-binding proteins,

TABLE 6B
Candidates Selected from TMT2 and LFQ2 Datasets

		TMT2		LFQ2	
Accession	Description	Abundance ratio: (24 h)/(0 h)	Abundance ratio P value: (24 h)/(0 h)	Abundance ratio: (24 h)/(0 h)	Abundance ratio P value: (24 h)/(0 h)
P02741	C-reactive protein	2.1	1,05E-05	2.049	1,16E-04
PO0DUB6	Alpha-amylase 1A	3.326	1,80E-13	100.00	1,00E-17
P11226	Mannose-binding protein C	1.229	3,35E-01	1.213	2,99E-01
P55058	Phospholipid transfer protein	1.494	2,65E-02	1.543	1,98E-02
P01031	Complement C5	1.586	9,27E-03	1.494	3,11E-02
P24592	Insulin-like growth factor-binding protein 6	1.35	1,18E-01	1.281	1,83E-01
P04114	Apolipoprotein B-100	1.219	3,63E-01	1.225	2,75E-01
Q13790	Apolipoprotein F	1.341	1,28E-01	1.543	1,97E-02
P61626	Lysozyme C	0.77	4,11E-02	0.654	2,22E-02
P18428	Lipopolysaccharide-binding protein	1.406	6,77E-02	1.585	1,33E-02
001459	Di-N-acetylchitobiase	1.242	3,03E-01	1.431	1,19E-01
075636	Ficolin-3	1.419	5,91E-02	1.377	8,56E-02
P29622	Kallistatin	1.215	3,74E-01	1.234	2,59E-01
P04070	Vitamin K-dependent protein C	1.261	2,60E-01	1.234	2,59E-01
Q15848	Adipoctin	1.269	2,43E-01	0.946	7.63E-01

Notes. Overview of 15 candidates selected from TMT2 and LFQ2 datasets based on ratio of the values at 0 h and 24 h postirradiation. The threshold value of abundance ratio was set as higher than 1.21 or lower than 0.89-fold ($P \leq 0.05$).

apolipoprotein B-100 and F, lysozyme C, lipopolysaccharide binding protein, di-N-acetylchitobiase, ficolin 3, kallistatin, protein C, and adiponectin. According to the available literature, some of these have been already reported in association with a radiation-induced response in vivo.

Insulin-like growth factor-binding proteins (IGFBPs) are involved in the regulation of insulin-like growth factor (IGF)-mediated signal transduction and thus can profoundly influence cellular phenotypes and cell fate (*50*). Several studies have established the association of the IGF pathway with radiation (*51*). For example, analysis of non-irradiated and irradiated mice showed that radiosensitivity and survival after irradiation are related to, among other things, the state of tissue activation and systemic IGF-1 signaling. Thus, exposure to radiation leads to the activation of several IGF-1 receptor tyrosine kinases involved in the radiation-induced response to DNA damage (*52*). IGFBP family proteins are closely associated with the inflammatory response and are involved in the removal of superoxides and radiation-damaged cells. In these conditions, their plasma levels increase similarly as in our study. In this context, our results confirm their role in TBI response and also implicate the importance of radiosensitivity.

The next identified candidates apolipoprotein B-100 and apolipoprotein F are involved in lipid metabolism (*53*). Elevated plasma level of apolipoprotein B-100 is a strong risk factor for the development of premature atherosclerotic disease induced by radiation (*54*). Furthermore, apolipoprotein F is known to be a lipid transfer inhibitor ex vivo (*55*).

Lysozyme C is a glycosidase found in various types of tissues, i.e., plasma, saliva, liver, and articular cartilage, and is characterized by its antibacterial capacity (*56*). When the lysozyme protein is irradiated, the structure is disrupted and the total amount of enzyme in plasma is decreased (*57*). Franzini et al. observed that the hydroxyl radical OH and secondary free radicals caused changes in lysozyme with subsequent aggregation. Furthermore, lysozyme activity decreased rapidly with the magnitude of the radiation dose (*58*). The decrement in plasma lysozyme levels was also confirmed in this study.

Lipopolysaccharide binding protein (LBP) is an acute phase protein and its levels increase significantly during systemic inflammatory reactions and sepsis. Its secretion is induced by IL-1 or IL-6 (*59*). The results of Chalubinska-Fendler et al. showed its dose-dependent association with radiation in the lung tissue (*60*). More specifically, increased levels of LBP were observed in 51 cancer patients 24 h after irradiation (*61*).

Ficolin 3 and mannose-binding lectin (MBL) in conjunction with MBL/Ficolin-associated serine proteases (MASPs) are the initiating molecules of the lectin pathway (*62*). Ficolin-3 serum level increases during inflammatory and infectious conditions (*63*). To the best of our knowledge, this is the first report associating ficolin 3 with radiation exposure, as its expression was increased of up to 1.4-fold in the performed experiments.

Kallistatin is a plasma protein that inhibits apoptosis and oxidative stress, thereby regulating the negative effects of radiation-induced products in vivo (*64*). The administration of kallistatin via gene transfer attenuated ROS production and organ damage due to oxidative stress (*65*). A slight increase in kallistatin expression was also observed in TBI

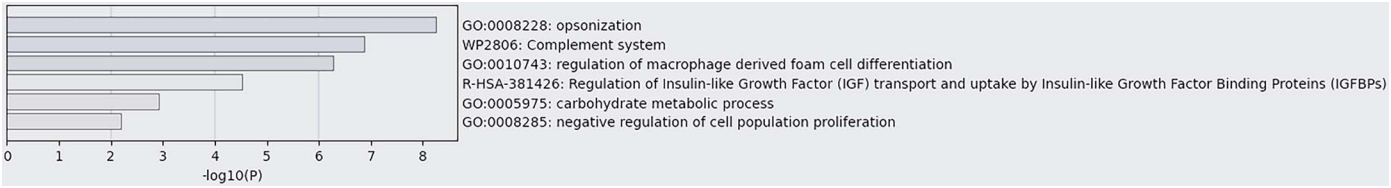

FIG. 1. Overview of signaling pathways in which the dysregulated proteins are involved.

samples analyzed in this study, where an increased presence of ROS was anticipated.

Vitamin K-dependent Protein C is a glycoprotein acting as an anticoagulant (*66*). A direct link to radiation has not been reported in the radiobiological literature, thus it would be an interesting candidate for further investigation, nevertheless the increase we observed was only modest.

Adiponectin is one of the cytokines that positively responds to oxidative stress and its properties allow it to regulate tissue damage and repair after irradiation (*67*). A relationship between plasma levels of adiponectin and inflammatory markers such as CRP has been previously demonstrated (*68*). There was a slight increase in plasma adiponectin levels observed in this study. The same result was obtained in another study, in which 16 male rhesus macaques were irradiated with 4 Gy (*69*).

In summary, this experimental study describes potential irradiation biomarkers after total-body irradiation. Despite the cohort was limited to 16 TBI patients, another batch of patients is currently being sampled to validate these data.

Most of the proteomic biomarkers studies published so far used animal models (pigs, rats, mice, non-human primates) and not humans. In the case of studies performed on human plasma, the irradiation was performed in vitro after the blood collection, which might result in a different biological response than in vivo. On the other hand, we have used human plasma from leukemia patients, who have undergone TBI as a part of their therapy. Naturally, this also represents a certain limitation due to their condition. We believe that the most significant contribution is the data obtained from human plasma irradiated in vivo, which further deepens the knowledge of proteomic biomarkers for practical biodosimetry. Moreover, two independent mass-spectrometry strategies were applied to increase data reliability. Above all, the results from our study also correlate well with the radiobiology literature underlining the importance and applicability of our candidate biomarkers. The majority of identified proteins were found to be associated with the acute radiation response (suggesting low probability of artefacts and confirming the biological relevance).

When evaluating our data in regard to other radiation biomarker publications, despite our efforts we did not find a comparable study to ours on TBI patients. Nevertheless, as mass spectrometry is a fast and sensitive analytical technique that has found application in the discovery of proteomic markers, we managed to find partially similar publications using proteomic approach on animal models. Surprisingly, the results were similar in the terms of the fold-change pattern for the top five proteomic candidates. Following publications report increase after exposure of different organisms for these proteins: CRP (*32*), AMY1A (*34*, *70*), PLPT (*39*), C5 (*71*) and MBL (*48*, *49*). In Table 7, there is a comparison of fold differences of the selected proteomic biomarkers identified in this study with other publications and some values are fairly comparable (e.g., for CRP).

The future steps will involve validating the suggested proteomic biomarkers on a larger cohort (with different age, sex, disease, or lifestyle), and developing a detection strategy, possibly based on immunochemical methods such as ELISA. Finally, the implementing into the clinical settings should follow once the benefit to the patient is proved. It is worth mentioning that for all protein candidates identified in our study (AMY1A, C5, PLPT, and MBL), a commercial kit is already available, but it is not used routinely. Besides, CRP is included in standard biochemical screening in the hospitals e.g., for cardiovascular risk discrimination (*72*).

In conclusion, the present study focused on the discovery of radiation biomarkers in the plasma of TBI leukemia

TABLE 7
Comparison Fold Differences in the Selected Proteomic Biomarkers

Protein	Mean fold change	Reference	Organism	Dose (Gy)	Biological material	Methods	Fold change
CRP	1.74	(*32*)	rhesus macaques	3.5	plasma	ELSIA	3.8
AMYIA	2.00	(*37*)	rhesus macaques	6.5	plasma	ELISA	1.9
PLPT	1.34	(*39*)	rats	3.5	plasma	MS	1.5
C5	1.40	(*71*)	mice	8.0	cells	ELISA	upregulated
MBL	1.41	(*48*)	mice	111.0	serum	IMS	11.5

Notes. The comparison the fold differences in the top 5 selected proteomic biomarkers with other published fold differences for comparable radiation exposures.

patients. Several differentially regulated plasma proteins were identified and quantified prior to and 24 h postirradiation. Comparing the obtained results with a control group yielded a list of candidates with a demonstrable association with radiation exposure.

Most of these candidates were related with the immune response (e.g. opsonization and complement system activation) typically associated with irradiated patients (*73*), and in which a variety of signaling pathways is triggered. It must be mentioned that the causal link between radiation exposure and complement activation has been historically demonstrated (*74*). Interestingly, lipid metabolism was dysregulated in the evaluated patients too. Taken together, the performed study provides biologically relevant findings not only for biodosimetry purposes but for radiation biology in general and presents a platform for future studies on radiation biomarkers in humans.

ACKNOWLEDGMENTS

This work was supported by the Ministry of Education, Sport and Youth (Specific research project 2108 - University of Hradec Kralove) and the Ministry of Defence of the Czech Republic (Long-term Development Plan of the University of Defence, Faculty of Military Health Sciences Hradec Kralove, Czech Republic – Medical issues of WMD II, DZRO-FVZ22-ZHN II).

Received: July 21, 2023; accepted: December 12, 2023; published online: February 5, 2024

REFERENCES

1. Sullivan JM, Prasanna PGS, Grace MB, Wathen L, Wallace RL, Koerner JF, et al. Assessment of Biodosimetry Methods for a Mass-Casualty Radiological Incident: Medical Response and Management Considerations. Health Phys [Internet]. 2013 Dec [cited 2020 Oct 12];105(6). Available from: https://www.ncbi.nlm.nih.gov/pmc/articles/PMC3810609/
2. Chaudhry MA. Biomarkers for human radiation exposure. J Biomed Sci. 2008 Sep 1;15(5):557–63.
3. Zeegers D, Venkatesan S, Koh SW, Low GKM, Srivastava P, Sundaram N, et al. Biomarkers of Ionizing Radiation Exposure: A Multiparametric Approach. Genome Integr [Internet]. 2017 Jan 23 [cited 2018 Dec 10];8. Available from: https://www.ncbi.nlm.nih.gov/pmc/articles/PMC5320786/
4. Mukherjee S, Laiakis EC, Fornace AJ, Amundson SA. Impact of inflammatory signaling on radiation biodosimetry: mouse model of inflammatory bowel disease. BMC Genomics [Internet]. 2019 May 2 [cited 2020 Oct 12];20. Available from: https://www.ncbi.nlm.nih.gov/pmc/articles/PMC6498469/
5. Coleman CN, Koerner JF. Biodosimetry: Medicine, Science, and Systems to Support the Medical Decision-Maker Following a Large Scale Nuclear or Radiation Incident. Radiat Prot Dosimetry. 2016 Dec;172(1–3):38–46.
6. Swartz HM, Flood AB, Williams BB, Dong R, Swarts SG, He X, et al. Electron paramagnetic resonance dosimetry for a large-scale radiation incident. Health Phys. 2012 Sep;103(3):255–67.
7. Fliedner TM, Powles R, Sirohi B, Niederwieser D, European Group for Blood and Marrow Transplantation (EBMT) Nuclear Accident Committee (NAC). Radiologic and nuclear events: the METREPOL severity of effect grading system. Blood. 2008 Jun 15;111(12):5757–8; author reply 5758-5759.
8. Huang J, Qi Z, Chen M, Xiao T, Guan J, Zhou M, et al. Serum amyloid A1 as a biomarker for radiation dose estimation and lethality prediction in irradiated mouse. Ann Transl Med [Internet]. 2019 Dec [cited 2020 Oct 13];7(23). Available from: https://www.ncbi.nlm.nih.gov/pmc/articles/PMC6990035/
9. Ha CT, Li XH, Fu D, Moroni M, Fisher C, Arnott R, et al. Circulating Interleukin-18 as a Biomarker of Total-Body Radiation Exposure in Mice, Minipigs, and Nonhuman Primates (NHP). PLoS One [Internet]. 2014 Oct 7 [cited 2020 Oct 13];9(10). Available from: https://www.ncbi.nlm.nih.gov/pmc/articles/PMC4188589/
10. Wang J, Shao L, Hendrickson HP, Liu L, Chang J, Luo Y, et al. Total Body Irradiation in the "Hematopoietic" Dose Range Induces Substantial Intestinal Injury in Non-Human Primates. Radiat Res. 2015 Nov;184(5):545–53.
11. Singh VK, Newman VL, Romaine PL, Hauer-Jensen M, Pollard HB. Use of biomarkers for assessing radiation injury and efficacy of countermeasures. Expert Rev Mol Diagn. 2016 Jan 2;16(1):65–81.
12. Mayo T, Haderlein M, Schuster B, Wiesmüller A, Hummel C, Bachl M, et al. Is in vivo and ex vivo irradiation equally reliable for individual Radiosensitivity testing by three colour fluorescence in situ hybridization? Radiat Oncol [Internet]. 2019 Dec 31 [cited 2020 Oct 13];15. Available from: https://www.ncbi.nlm.nih.gov/pmc/articles/PMC6938618/
13. Pannkuk EL, Laiakis EC, Authier S, Wong K, Fornace AJ. Global Metabolomic Identification of Long-Term Dose-Dependent Urinary Biomarkers in Nonhuman Primates Exposed to Ionizing Radiation. Radiat Res. 2015 Aug;184(2):121–33.
14. Hoffmann W, Schmitz-Feuerhake I. How radiation-specific is the dicentric assay? J Expo Sci Environ Epidemiol. 1999 Apr;9(2):113–33.
15. Agency IAEA, Organization PAH, Organization WH. Cytogenetic Dosimetry: Applications in Preparedness for and Response to Radiation Emergencies [Internet]. International Atomic Energy Agency; 2011 [cited 2020 Oct 12]. Report No.: EPR-BIODOSIMETRY–2011. Available from: https://inis.iaea.org/Search/search.aspx?orig_q=RN:43025992
16. Lee Y, Jin YW, Wilkins RC, Jang S. Validation of the dicentric chromosome assay for radiation biological dosimetry in South Korea. J Radiat Res. 2019 Oct;60(5):555–63.
17. DiCarlo AL, Maher C, Hick JL, Hanfling D, Dainiak N, Chao N, et al. Radiation injury after a nuclear detonation: medical consequences and the need for scarce resources allocation. Disaster Med Public Health Prep. 2011 Mar;5 Suppl 1:S32-44.
18. Lacombe J, Sima C, Amundson SA, Zenhausern F. Candidate gene biodosimetry markers of exposure to external ionizing radiation in human blood: A systematic review. PLoS One [Internet]. 2018 Jun 7 [cited 2018 Dec 10];13(6). Available from: https://www.ncbi.nlm.nih.gov/pmc/articles/PMC5991767/
19. Hengel SM, Aldrich JT, Waters KM, Pasa-Tolic L, Stenoien DL. Quantitative Proteomic Profiling of Low-Dose Ionizing Radiation Effects in a Human Skin Model. Proteomes. 2014 Jul 29;2(3):382–98.
20. Wiśniewski JR, Gaugaz FZ. Fast and Sensitive Total Protein and Peptide Assays for Proteomic Analysis. Anal Chem. 2015 Apr 21;87(8):4110–6.
21. Ondrej M, Rehulka P, Rehulkova H, Kupcik R, Tichy A. Fractionation of Enriched Phosphopeptides Using pH/Acetonitrile-Gradient-Reversed-Phase Microcolumn Separation in Combination with LC–MS/MS Analysis. Int J Mol Sci. 2020 Jun 1;21(11):3971.
22. Perez-Riverol Y, Bai J, Bandla C, García-Seisdedos D, Hewapathirana S, Kamatchinathan S, et al. The PRIDE database resources in 2022: a hub for mass spectrometry-based proteomics evidences. Nucleic Acids Res. 2022 Jan 7;50(D1):D543–52.
23. Kim D, Marchetti F, Chen Z, Zaric S, Wilson RJ, Hall DA, et al. Nanosensor dosimetry of mouse blood proteins after exposure to ionizing radiation. Sci Rep. 2013;3:2234.
24. Blakely WF, Port M, Abend M. Early-response multiple-parameter biodosimetry and dosimetry: risk predictions. J Radiol Prot. 2021 Dec;41(4):R152.

25. Gnanasekaran TS. Cytogenetic biological dosimetry assays: recent developments and updates. Radiat Oncol J. 2021 Sep; 39(3):159–66.
26. Cengiz M, Akbulut S, Atahan IL, Grigsby PW. Acute phase response during radiotherapy. Int J Radiat Oncol Biol Phys. 2001 Mar 15;49(4):1093–6.
27. Nigam S, Schewe T. Phospholipase A(2)s and lipid peroxidation. Biochim Biophys Acta. 2000 Oct 31;1488(1–2):167–81.
28. Loganathan S, Athalye SN, Joshi SR. Itolizumab, an anti-CD6 monoclonal antibody, as a potential treatment for COVID-19 complications. Expert Opin Biol Ther. 2020 Sep;20(9):1025–31.
29. Ryu JW, Jung IH, Park EY, Kim KH, Kim K, Yeom J, et al. Radiation-induced C-reactive protein triggers apoptosis of vascular smooth muscle cells through ROS interfering with the STAT3/Ref-1 complex. J Cell Mol Med. 2022 Apr;26(7):2104–18.
30. Li JJ, Fang CH. C-reactive protein is not only an inflammatory marker but also a direct cause of cardiovascular diseases. Med Hypotheses. 2004;62(4):499–506.
31. Ki Y, Kim W, Nam J, Kim D, Park D, Kim D. C-reactive protein levels and radiation-induced mucositis in patients with head-and-neck cancer. Int J Radiat Oncol Biol Phys. 2009 Oct 1;75(2):393–8.
32. Ossetrova NI, Sandgren DJ, Blakely WF. C-reactive protein and serum amyloid A as early-phase and prognostic indicators of acute radiation exposure in nonhuman primate total-body irradiation model. Radiation Measurements. 2011 Sep 1;46(9):1019–24.
33. Janeček Š, Svensson B, MacGregor EA. α-Amylase: an enzyme specificity found in various families of glycoside hydrolases. Cell Mol Life Sci. 2014 Apr;71(7):1149–70.
34. Becciolini A, Giannardi G, Cionini L, Porciani S, Fallai C, Pirtoli L. Plasma amylase activity as a biochemical indicator of radiation injury to salivary glands. Acta Radiol Oncol. 1984;23(1):9–14.
35. Hofmann R, Schreiber GA, Willich N, Westhaus R, Bögl KW. Increased serum amylase in patients after radiotherapy as a probable bioindicator for radiation exposure. Strahlenther Onkol. 1990 Oct;166(10):688–95.
36. Blakely WF, Ossetrova NI, Manglapus GL, Salter CA, Levine IH, Jackson WE, et al. Amylase and blood cell-count hematological radiation-injury biomarkers in a rhesus monkey radiation model—use of multiparameter and integrated biological dosimetry. Radiation Measurements. 2007 Jul 1;42(6):1164–70.
37. Wirtz Karel WA. Phospholipid transfer proteins revisited. Biochemical Journal. 1997 Jun 1;324(2):353–60.
38. Parasassi T, Giusti AM, Gratton E, Monaco E, Raimondi M, Ravagnan G, et al. Evidence for an Increase in Water Concentration in Bilayers after Oxidative Damage of Phospholipids Induced by Ionizing Radiation. International Journal of Radiation Biology. 1994 Jan;65(3):329–34.
39. Wang C, Yang J, Nie J. Plasma phospholipid metabolic profiling and biomarkers of rats following radiation exposure based on liquid chromatography–mass spectrometry technique. Biomedical Chromatography. 2009;23(10):1079–85.
40. Pangburn MK, Rawal N. Structure and function of complement C5 convertase enzymes. Biochemical Society Transactions. 2002 Nov 1;30(6):1006–10.
41. Jore MM, Johnson S, Sheppard D, Barber NM, Li YI, Nunn MA, et al. Structural basis for therapeutic inhibition of complement C5. Nat Struct Mol Biol. 2016 May;23(5):378–86.
42. Fausto N, Campbell JS, Riehle KJ. Liver regeneration. Hepatology. 2006;43(S1):S45–53.
43. Jirtle RL, Michalopoulos G, McLain JR, Crowley J. Transplantation System for Determining the Clonogenic Survival of Parenchymal Hepatocytes Exposed to Ionizing Radiation1. Cancer Research. 1981 Sep 1;41(9_Part_1):3512–8.
44. Schieferdecker HL, Schlaf G, Koleva M, Götze O, Jungermann K. Induction of functional anaphylatoxin C5a receptors on hepatocytes by in vivo treatment of rats with IL-6. J Immunol. 2000 May 15;164(10):5453–8.
45. Strainic MG, Liu J, Huang D, An F, Lalli PN, Muqim N, et al. Locally Produced Complement Fragments C5a and C3a Provide Both Costimulatory and Survival Signals to Naive CD4+ T Cells. Immunity. 2008 Mar 14;28(3):425–35.
46. Surace L, Lysenko V, Fontana AO, Cecconi V, Janssen H, Bicvic A, et al. Complement Is a Central Mediator of Radiotherapy-Induced Tumor-Specific Immunity and Clinical Response. Immunity. 2015 Apr 21;42(4):767–77.
47. Collard CD, Montalto MC, Reenstra WR, Buras JA, Stahl GL. Endothelial Oxidative Stress Activates the Lectin Complement Pathway: Role of Cytokeratin 1. The American Journal of Pathology. 2001 Sep 1;159(3):1045–54.
48. Rosen E, Fatanmi OO, Wise SY, Rao VA, Singh VK. Gamma-tocotrienol, a radiation countermeasure, reverses proteomic changes in serum following total-body gamma irradiation in mice. Sci Rep. 2022 Mar 1;12(1):3387.
49. Rithidech KN, Honikel L, Rieger R, Xie W, Rithidech KN, Honikel L, et al. Protein-expression profiles in mouse blood-plasma following acute whole-body exposure to 137Cs γ rays. International Journal of Radiation Biology. 2009 Jan 1; 85(5):432–47.
50. Taferner A, Micutkova L, Hermann M, Jansen-Dürr P, Pircher H. Purification and characterization of native human insulin-like growth factor binding protein-6. J Cell Commun Signal. 2011 Dec;5(4):277–89.
51. Mylonas PG, Matsouka PT, Papandoniou EV, Vagianos C, Kalfarentzos F, Alexandrides TK. Growth hormone and insulin-like growth factor I protect intestinal cells from radiation induced apoptosis. Molecular and Cellular Endocrinology. 2000 Feb 25;160(1):115–22.
52. Zinati-Saeed S, Shakiba E, Rahimi Z, Akbari M, Najafi F, Bahrehmand F, et al. The Insulin-like Growth Factor-1 (G>A) and 5,10-methylenetetrahydrofolate Reductase (C677T) Gene Variants and the Serum Levels of Insulin-like Growth Factor-1, Insulin, and Homeostasis Model Assessment in Patients with Acne Vulgaris. Iran J Pathol. 2020;15(1):23–9.
53. Segrest JP, Garber DW, Brouillette CG, Harvey SC, Anantharamaiah GM. The Amphipathic α Helix: A Multifunctional Structural Motif in Plasma Apolipoproteins. In: Anfinsen CB, Edsall JT, Richards FM, Eisenberg DS, editors. Advances in Protein Chemistry [Internet]. Academic Press; 1994 [cited 2023 Feb 5]. p. 303–69. (Lipoproteins, Apolipoproteins, and Lipases; vol. 45). Available from: https://www.sciencedirect.com/science/article/pii/S0065323308606439
54. Young SG. Recent progress in understanding apolipoprotein B. Circulation. 1990 Nov;82(5):1574–94.
55. Lagor WR, Brown RJ, Toh SA, Millar JS, Fuki IV, de la Llera-Moya M, et al. Overexpression of Apolipoprotein F Reduces HDL Cholesterol Levels In Vivo. Arteriosclerosis, Thrombosis, and Vascular Biology. 2009 Jan;29(1):40–6.
56. Reitamo S, Klockars M, Adinolfi M, Osserman EF. Human lysozyme (origin and distribution in health and disease). Ric Clin Lab. 1978;8(4):211–31.
57. Edwards AM, Ruiz M, Silva E, Lissi E. Lysozyme modification by the fenton reaction and gamma radiation. Free Radic Res. 2002 Mar;36(3):277–84.
58. Franzini E, Sellak H, Hakim J, Pasquier C. Oxidative damage to lysozyme by the hydroxyl radical: comparative effects of scavengers. Biochim Biophys Acta. 1993 Nov 10;1203(1):11–7.
59. Jack RS. CD14 in the Inflammatory Response. Karger Medical and Scientific Publishers; 2000. 191 p.
60. Chalubinska-Fendler J, Fendler W, Spych M, Wyka K, Luniewska-Bury J, Fijuth J. Lipopolysaccharide-binding protein is efficient in biodosimetry during radiotherapy of lung cancer. Biomed Rep. 2016 Oct;5(4):450–4.
61. Chalubinska-Fendler J, Graczyk L, Piotrowski G, Wyka K, Nowicka Z, Tomasik B, et al. Lipopolysaccharide-Binding Protein Is an Early Biomarker of Cardiac Function After Radiation

Therapy for Breast Cancer. International Journal of Radiation Oncology*Biology*Physics. 2019 Aug;104(5):1074–83.

62. Thiel S. Complement activating soluble pattern recognition molecules with collagen-like regions, mannan-binding lectin, ficolins and associated proteins. Molecular Immunology. 2007 Sep 1; 44(16):3875–88.

63. Hein E, Honoré C, Skjoedt MO, Munthe-Fog L, Hummelshøj T, Garred P. Functional Analysis of Ficolin-3 Mediated Complement Activation. PLOS ONE. 2010 11;5(11):e15443.

64. Shen B, Smith RS, Hsu YT, Chao L, Chao J. Kruppel-like Factor 4 Is a Novel Mediator of Kallistatin in Inhibiting Endothelial Inflammation via Increased Endothelial Nitric-oxide Synthase Expression. J Biol Chem. 2009 Dec 18;284(51):35471–8.

65. Gao L, Yin H, S Smith R, Chao L, Chao J. Role of kallistatin in prevention of cardiac remodeling after chronic myocardial infarction. Lab Invest. 2008 Nov;88(11):1157–66.

66. Wypasek E, Undas A. Protein C and protein S deficiency - practical diagnostic issues. Adv Clin Exp Med. 2013;22(4):459–67.

67. Ponemone V, Fayad R, Gove ME, Pini M, Fantuzzi G. Effect of adiponectin deficiency on intestinal damage and hematopoietic responses of mice exposed to gamma radiation. Mutat Res. 2010 Aug 7;690(1–2):102–7.

68. Ouchi N, Walsh K. Adiponectin as an anti-inflammatory factor. Clin Chim Acta. 2007 May 1;380(1–2):24–30.

69. Bacarella N, Ruggiero A, Davis AT, Uberseder B, Davis MA, Bracy DP, et al. Whole Body Irradiation Induces Diabetes and Adipose Insulin Resistance in Nonhuman Primates. International Journal of Radiation Oncology*Biology*Physics. 2020 Mar; 106(4):878–86.

70. Leslie MD, Dische S. Changes in serum and salivary amylase during radiotherapy for head and neck cancer: a comparison of conventionally fractionated radiotherapy with CHART. Radiother Oncol. 1992 May;24(1):27–31.

71. Yuan M, Wang C, Wu Y, Qiao L, Deng G, Liang N, et al. Targeting complement C5a to improve radiotherapy sensitivity in non-small cell lung cancer. Transl Lung Cancer Res. 2023 May 31;12(5):1093–107.

72. Ridker PM. Clinical application of C-reactive protein for cardiovascular disease detection and prevention. Circulation. 2003 Jan 28;107(3):363–9.

73. McKelvey KJ, Hudson AL, Back M, Eade T, Diakos CI. Radiation, inflammation and the immune response in cancer. Mamm Genome. 2018 Dec 1;29(11):843–65.

74. Regal JF, Dornfeld KJ, Fleming SD. Radiotherapy: killing with complement. Ann Transl Med. 2016 Mar;4(5):94.